DELTA JOURNAL OF SCIENCE 2005, 29, 18-38

MINERALOGY AND URANIUM DISTRIBUTION IN SOME SUBSURFACE SECTIONS FROM EL-MISSIKAT AND EL-EREDIYA URANIUM OCCURRENCES, EASTERN DESERT, EGYPT.

OSMAN, A. M. *, SALMAN, A. B. **, EL-MANSI, M. M. **, ABDEL GHANI, I. M. **, ABDALLAH, S. M. **

* FACULTY OF SCIENCE, AIN SHAMS UNIVERSITY

** NUCLEAR MATERIALS AUTHORITY, CAIRO, EGYPT

(Received: 19 February, 2005)

ABSTRACT

Twelve boreholes were drilled, two at El-Missikat uranium occurrence and ten at El-Erediya uranium occurrence. Studying the two boreholes of El-Missikat area (MS-2 and MS-3) and four boreholes from El-Erediya area (Er-1, Er-4M-30, Er-7M-60 and Er-8M-90) reveals the presence of some high radioactive anomalies that are related to the main shear zones. Other lower radioactive anomalies are also recorded related to some fractures around the main shear zone. The radioactive anomalies are mainly related to uranium concentration and not to thorium concentration. They are not related to any of the fresh sulphide zones but mainly related to the goethite (pseudomorph after pyrite) zone. There is no general trend for increasing or decreasing of either uranium or thorium with depth for any of the studied boreholes. Also, the uranium mineralizations are of secondary nature and intimately related to shear zones and fracture system and accordingly to type and degree of alteration.

Uranothorite and cassiterite are only encountered in core samples at level more than 80 m depth (below the main adit level) of El-Erediya boreholes indicating a transitional area between the oxidation and reduction zones. They are not encountered in core samples at any depth of El-Missikat boreholes indicating oxidation zone till 150 m depth below the wadi level.

INTRODUCTION

El-Missikat and El-Erediya granitic plutons are located in the Central Eastern Desert of Egypt within the limits of latitudes 26° 18′ and 26° 30′ N and longitudes 33° 20′ and 33° 30′ E (Fig. 1). El-Missikat and El-Eredyia uranium occurrences were discovered by Bakhit (1978) and El-Kassas (1974), respectively. The geology of both El-Missikat and El-Erediya plutons were studied by several authors (Nagi, 1977, Abu Dief, 1985, Rabie and Ammar, 1992, El-Mansi, 1993, Abdallah, 1998 & 2004, Moharem, 2000, Raslan, 2001 and others). The present work deals with the geological, petrographical, mineralogical, geochemical and radiometrical studies on some subsurface sections from the radioactive mineralized granites of the two plutons.

Several sub-parallel shear zones trending nearly NE-SW dissect the northern part of El-Missikat pluton along its contact with the older granitoids (Fig.2a) and the southern part of El-Erediya pluton near its

ISSN 1012 – 5965

contact with the metavolcanics (Fig.2b). These shear zones are characterized by intensive kaolinization, silicification and ferrugination as well as the common presence of jasper and quartz.

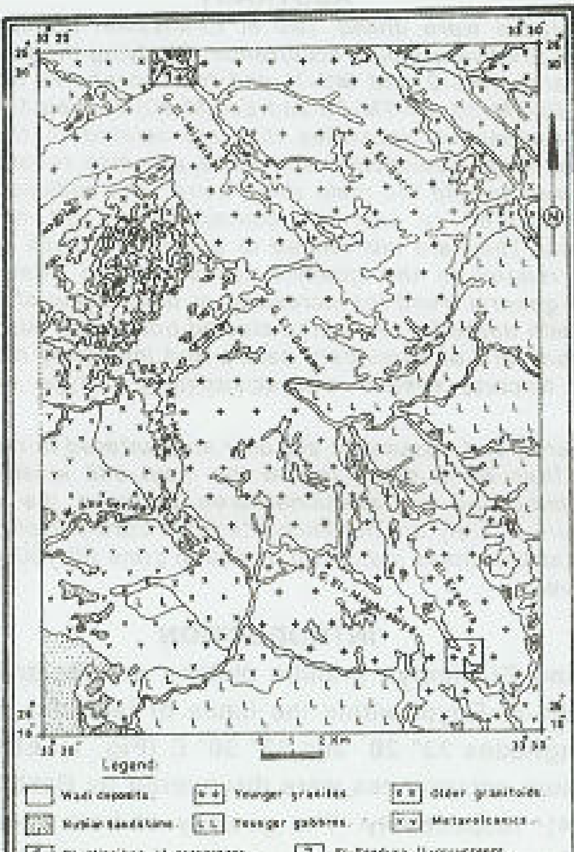

FIG. 1 : GEOLOGICAL MAP OF EL-MISSIKAT-EL-EREDIYA AREA, CENTRAL EASTERN DESERT, EGYPT.

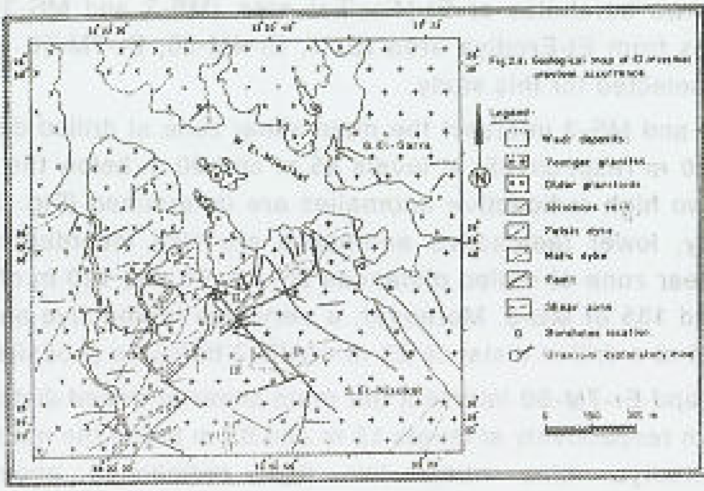

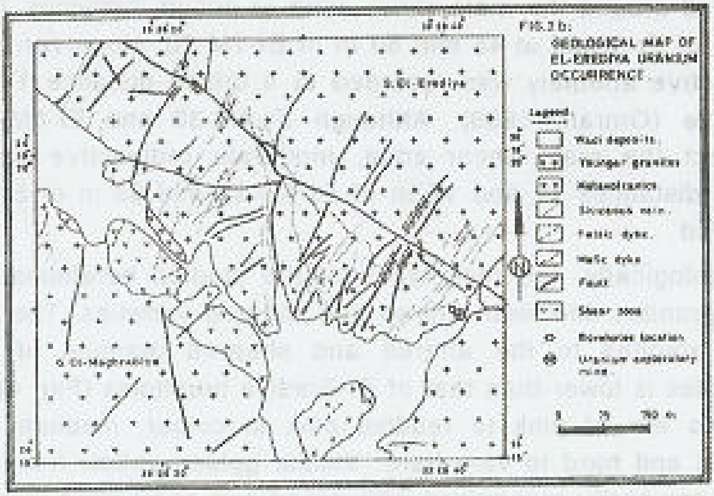

The jasperoid veins are characterized by abnormal radioactivity and their association of visible uranium mineralizations that concentrated as scattered yellow spots of uranophane and beta-uranophane.

SUBSURFACE INVESTIGATIONS

Drilling was used to explore the uranium bearing veins at deeper levels and obtain more geological data of El-Missikat and El-Erediya granites. A drilling program was recommended (Salman, 1995). Two types of drilling (Diamond core drilling and percussion drilling) were used for this purpose. Twelve boreholes were drilled, two at El-Missikat uranium occurrence and ten at El-Erediya uranium occurrence (Table 1). The two boreholes of El-Missikat area (MS-2 and MS-3) and four boreholes from El-Erediya area (Er-1, Er-4M-30, Er-7M-60 and Er-8M-90) are selected for this study.

MS-2 and MS-3 intersect the main shear zone at drilled distances 80 m and 90 m respectively at levels 45 m and 90 m below the wadi level where two high radioactive anomalies are determined (Fig. 3a). Other, relatively, lower radioactive anomalies are also recorded around the main shear zone at drilled distances 25, 43, 65 and 120 m of MS-2 and at 85 and 135 of MS-3. Moreover, a very high radioactive anomaly was recorded at a drilled distance 23 m of MS-2 borehole (Abdallah, 1998).

Er-1 and Er-7M-60 intersect the main shear at drilled distances 18 m and 89 m respectively at levels 15 m and 85 m below the main adit level of El-Erediya mine where two high radioactive anomalies are determined (Fig. 3b). Other lower radioactive anomalies are also recorded around the main shear zone at drilled distances 72, 101 and 139 m of Er-1 and at 45 and 80 m of Er-7M-70. Moreover, a moderate radioactive anomaly was recorded at a drilled distance 17 m of Er-1 borehole (Omran, 1999). Although Er-4M-30 and Er-8M-90 do not intersect the main shear zone, moderate radioactive anomalies at drilled distances 12 and 17 m of Er-4M-30 and 93 m of Er-8M-90 are recorded.

Lithologically, the rock types of the studied boreholes are mainly fresh granites and their altered and sheared varieties. The ratio of the fresh granites to the altered and sheared granites of El-Missikat boreholes is lower than that of El-Erediya boreholes (Fig. 4). The fresh granites are of pink to reddish pink in colour, medium- to coarse-grained and hard to very hard. Visible golden yellow fresh crystals of pyrite are easily recognized with naked eye or by hand lens in most of El-Erediya core samples at various depths. They are encountered as disseminations in the host fresh granite or in quartz veinlets cutting this granite.

The fresh granites are subjected to shearing and fracturing that show signs of alterations. Several types of alterations can be easily determined comprising kaolinization, silicification, ferrugination, carbonatization and chloritization. Staining of manganese oxides is also observed along the fracture planes.

Table (1): The constructed drilling program of El-Missikat and El-Erediya areas (Modified after Salman, 1995)

Area	Borehole name	Location	Plunging	Length (m)	Core drilling length (m)	Target
El-Missikat	*MS-2*	6 m south the northeastern mass	30° N20°W	135.50	131	The main shear zone at level 45 m from wadi level
	MS-3	8 m south the northeastern mass	Vertical	150.75	140.15	The main shear zone at level 90 m from wadi level
El-Erediya	*Er-1*	34.8 m inward from the portal	45° N45°W	176.40	Full coring	Shear zones II and III.
	Er-2M-30	35.1 m inward from the portal	72° N77°W	47.00	Full coring	Anomaly VI at level 30 m from the main adit level
	Er-3M-30	35.1 m inward from the portal	74° N08°W	42.00	Full coring	Anomaly V at level 30 m from the main adit level
	Er-4M-30	36.5 m inward from the portal	86° N45°W	40.70	Full coring	Spot anomalies at level 30 m from the main adit level
	Er-5M-60	0.7 m outward from the portal	64° N59°W	96.90	Full coring	Anomaly VI at level 60 m from the main adit level
	Er-6M-60	0.5 m outward from the portal	64° N26°W	90.75	Full coring	Anomaly V at level 60 m from the main adit level
	Er-7M-60	0.8 m outward from the portal	70° N45°W	100.80	Full coring	Spot anomalies at level 60 m from the main adit level
	Er-8M-90	2.8 m outward from the portal	80° N45°W	109.70	34.70	Spot anomalies at level 90 m from the main adit level
	Er-9M-90	2.7 m outward from the portal	76° N64°W	101.90	21.90	Anomaly VI at level 90 m from the main adit level
	Er-10M-90	2.8 m outward from the portal	75° N25°W	105.60	45.60	Anomaly V at level 90 m from the main adit level

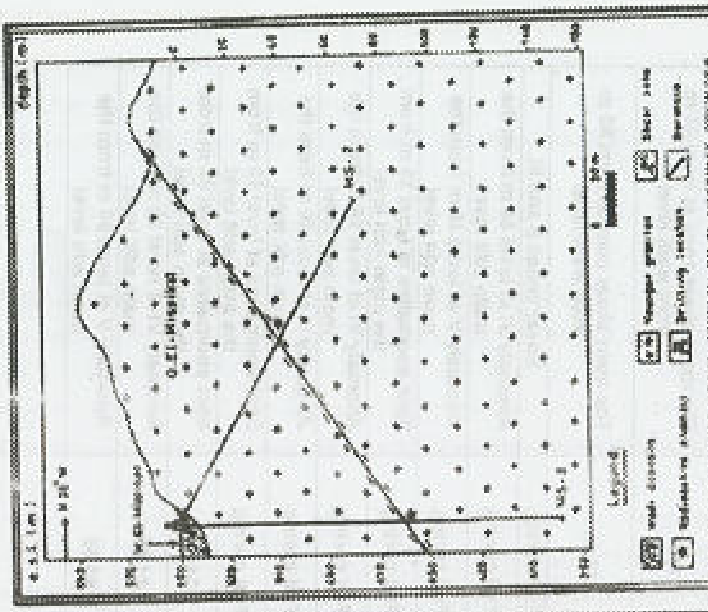

FIG. 3a. SCHEMATIC CROSS-SECTION OF EL-MISSIKAT YOUNGER GRANITES SHOWING THE LOCATION, ALTITUDE AND DEPTH OF THE STUDIED BOREHOLES.

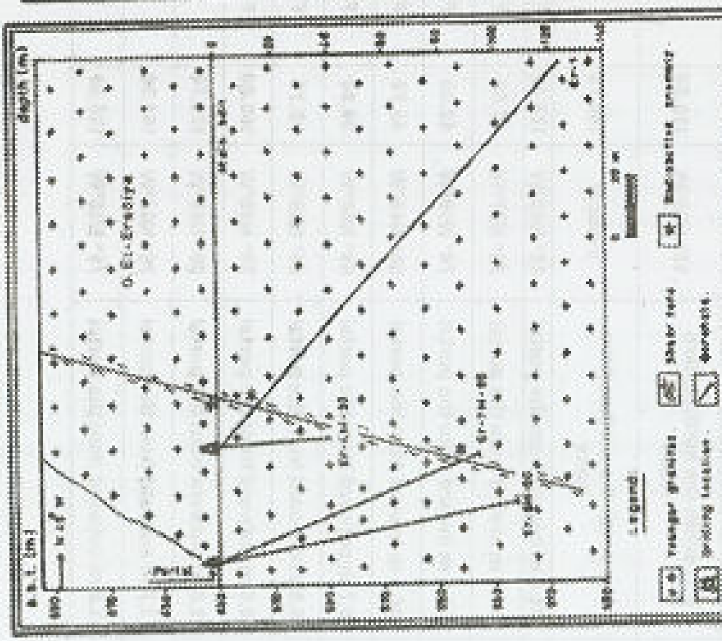

FIG. 3b. SCHEMATIC CROSS-SECTION OF EL-EREDIYA YOUNGER GRANITES SHOWING THE LOCATION, ALTITUDE AND DEPTH OF THE STUDIED BOREHOLES.

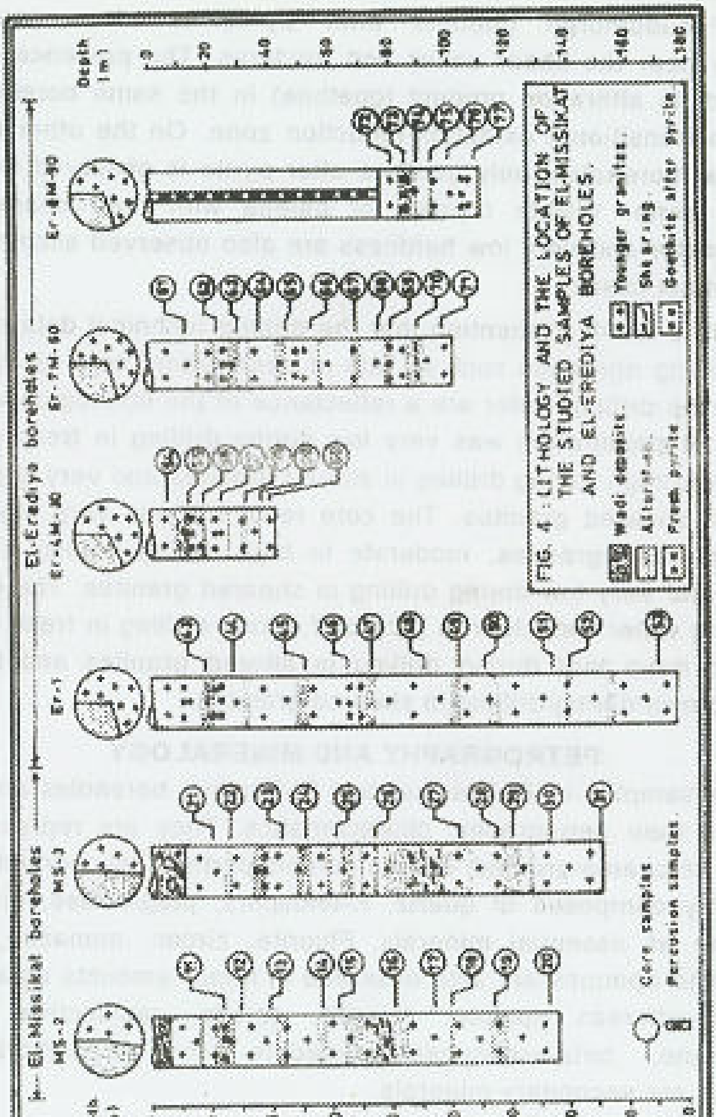

FIG. 4 : LITHOLOGY AND THE LOCATION OF THE STUDIED SAMPLES OF EL-MISSIKAT AND EL-EREDIYA BOREHOLES.

The intensity of alteration decreases gradually away from the shear zones. Pseudomorph goethite after pyrite is also encountered especially near the shear zones and fractures. The presence of fresh pyrite and its alteration product (goethite) in the same borehole may indicate a transitional oxidation-reduction zone. On the other hand, at El-Missikat boreholes, only goethite after pyrite is observed indicating oxidation zone. Visible crystals of galena with their characterized metallic luster and very low hardness are also observed accompanying pyrite in most cases.

Also, it is worth to mention that the drilling technical data collected during drilling operation such as rate of penetration, core recovery and colour of the drilling water are a reflectance of the lithologic variations. The rate of penetration was very low during drilling in fresh granites, moderate to high during drilling in altered granites and very high during drilling in sheared granites. The core recovery was very high during drilling in fresh granites, moderate to high during drilling in altered granites and very low during drilling in sheared granites. The colour of the drilling water was clear to pale buff during drilling in fresh granites, yellow to deep buff during drilling in altered granites and brown to reddish brown during drilling in sheared granites.

PETROGRAPHY AND MINERALOGY

The core samples of El-Missikat and El-Erediya boreholes are closely similar in their petrographic characteristics. They are represented by medium- to coarse-grained, allotriomorphic perthitic leucogranites. They are mainly composed of quartz, K-feldspars, plagioclase, biotite and muscovite as essential minerals. Fluorite, zircon, monazite, apatite, sphene and opaques are also observed in minor amounts as accessory minerals whereas epidote, chlorite, calcite, radioactive minerals (uranophane, beta-uranophane, kasolite and uranothorite) and cassetrite are secondary minerals.

The altered samples are mostly fractured and brecciated with clear porphyroclastic texture. They are medium- to coarse- grained, hypidiomorphic and composed of jasper, quartz, perthites, plagioclase and subordinate amount of mica (biotite and muscovite) as essential minerals. The accessory minerals are rare and mainly represented by zircon and apatite crystals. The secondary minerals are mainly represented by fluorite, kaolinite, sericite, chlorite and epidote, iron oxides as well as uranium minerals.

The mineralized samples show high quartz content (reach up 85%) with uranium mineralization. The increase in secondary quartz is accompanied by a decrease in the perthites and plagioclase contents. Smoky quartz is a good evidence of radiogenic effect of the neighbouring uranium minerals. They show high contents of deep violet fluorite and metamict zircon as well as higher contents of iron oxides than those of fresh granites. Iron oxides are usually coated by a thin film of secondary uranium mineralization. This may be attributed to the ability of iron oxides to adsorb uranium from the circulating hydrothermal solutions. The radioactive minerals are mainly represented by uranophane, beta- uranophane, kasolite and uranothorite.

Generally in both El-Missikat and El-Erediya boreholes, with increasing depth, the degree of alteration decreases and accordingly the amounts of secondary minerals such as fluorite, calcite and iron oxides also decrease. Sulphides also decreases with increasing depth. Biotite gets to be larger, fresher and clustered with increasing depth. Some pegmatitic samples with very large perthite, plagioclase and quartz crystals are noticed at depth at level not more than 40 m depth and disappear beyond this level. Uranothorite and cassiterite are only encountered in core samples at level more than 80 m depth of El-Erediya boreholes indicating a transitional area between the oxidation and reduction zones. On the other hand, they are not encountered in core samples at any depth of El-Missikat boreholes indicating oxidation zone till 150 m depth.

Uranophane and beta-uranophane (Figs. 5 A and B) are distinguished by their canary to lemon yellow colour. Reddish brown variety is also encountered. They are generally massive with granular form. Fibrous and radiating acicular crystals are also encountered (Figs. 5 C and D). They are characterized by their dull and/or greasy luster, their softness to crushing by pressing with picking needle and their pale yellow streak. No variations in the mineral XRD patterns (Fig. 6) are observed with respect to the colour or habit which may indicate that the colour of uranophane and beta-uranophane is due to the iron staining that caused by hydration of the associated magnetite and hematite.

Fluorite (Figs. 5 E and F) is common in the sheared mineralized granites and rare in the fresh host granites. The colours of fluorite vary from colourless, white, smoky, pale yellow, blue and violet. All the colour varieties have the same XRD pattern (Fig. 7). This may indicate that the colouration of fluorite is not related to any impurities but mostly connected with the irradiation by the associating uranium minerals (El-Mansi, 2000). Colourless fluorite is more dominant than the deep violet fluorite in the fresh samples and vice versa in the mineralized granites. The colourless fluorite appears as well developed transparent euhedral crystals of vitreous luster but the coloured fluorite occurs commonly as subheral to euhedral translucent crystals of vitreous and/or greasy luster.

Zircon from the fresh samples is mainly normal zircon of adamantine luster, but the separated zircon from the mineralized granites is represented by normal and metamict zircon (Figs. 8 A and B). Generally, zircon grains vary from transparent to opaque. Two types of zircon crystals are recorded. The first is water clear (common type), euhedral minute crystals reflecting their magmatic origin. The second type shows an effect of dissolution deduced from the necked crystals with somewhat zoning and corroded terminations. Inclusions within the zircon are of different shapes (spherical, fibrous and irregular) and different colours (colourless, red and brown) and are common in the second type, reflecting the effect of hydrothermal solutions. The magnetic zircon crystals are generally coated and stained with iron oxides which give the crystals their brownish colour and most of them contain inclusions. The magnetic susceptibility and colouration of zircon are directly proportional to the intensity of inclusions and/or iron staining. Accordingly, the water clear zircon concentrates in the non-magnetic fraction (1.5 ampere), while the coloured zircon is concentrated in the magnetic fraction (0.5 and 1 ampere).

In the mineralized granites, the necked zircon crystals are common, their edges and terminations are highly corroded suggesting an intense process of dissolution. The zircon crystals are predominantly brown or reddish brown in colour due to staining with iron oxides. Zonation and outgrowths are very common confirming the hydrothermal effect (Holten *et al.*, 2000 and De La Rosa *et al.*, 2002). Inclusions in zircon are highly common, which are considered as weak points that accelerate the disintegration of the grains during alteration processes. They are randomly distributed within the zircon crystals and are mainly represented by iron oxides. Fine inclusions are also present in zircon and give them the cloudy appearance. The water clear zircon is very rare or completely absent.

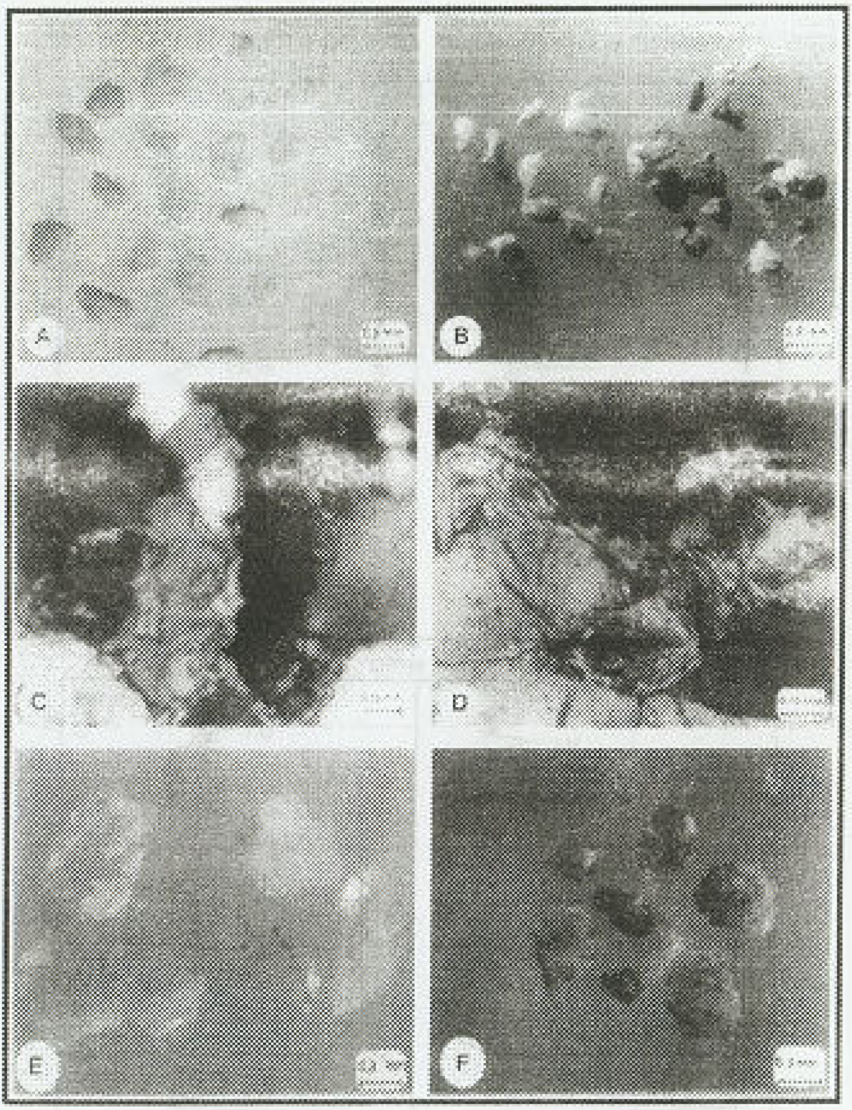

Fig. 5A: Canary yellow uranophane grains. Binocular microscope.

Fig. 5B: Lemon yellow and reddish brown massive uranophane and beta-uranophane grains. Binocular microscope.

Fig. 5C: Uranophane crystals interstitially between quartz and plagioclase. C.N.

Fig. 5D: Fibrous beta-uranophane crystals interstitially between quartz. C.N.

Fig. 5E: Colourless and white fluorite grains with brown inclusions. Binocular microscope.

Fig. 5F: Blue and smoky fluorite grains with black inclusions. Binocular microscope.

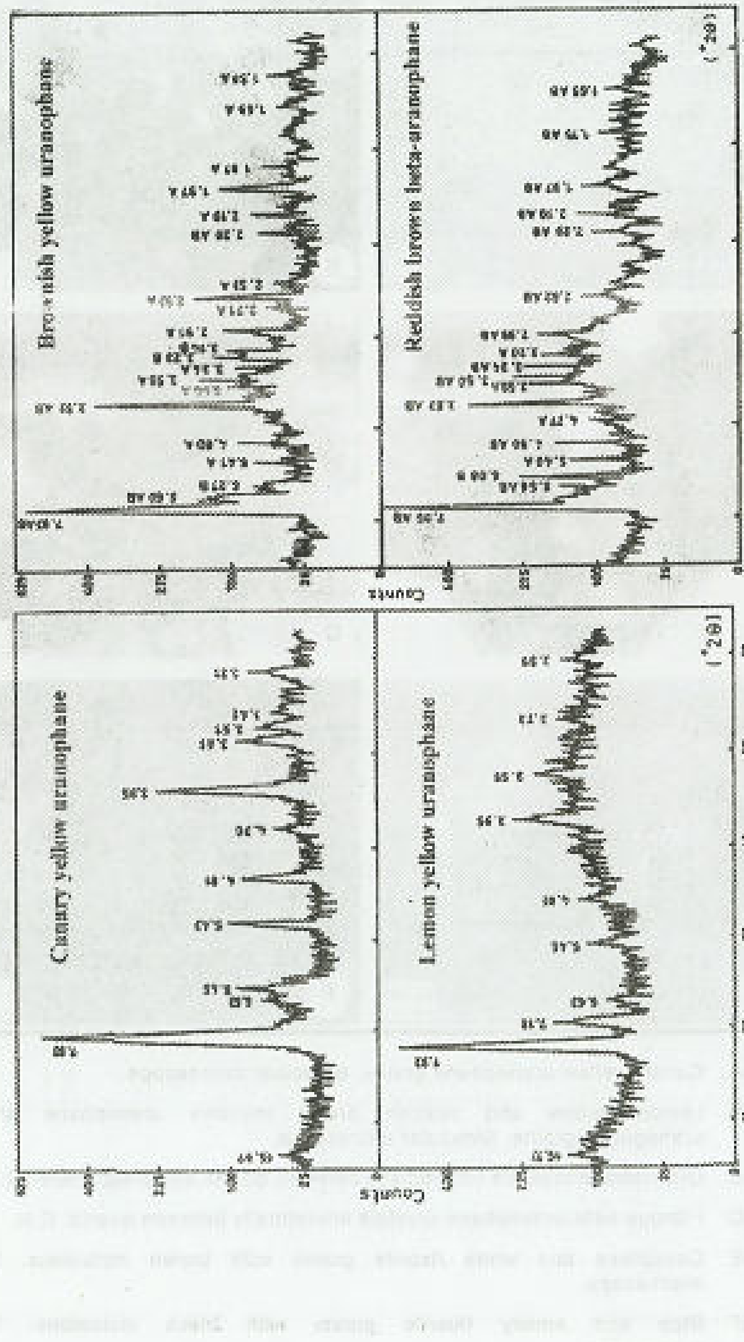

Fig.6: XRD charts for different varieties of uranophane and beta-uranophane, El-Missikat and El-Erediya plutons.

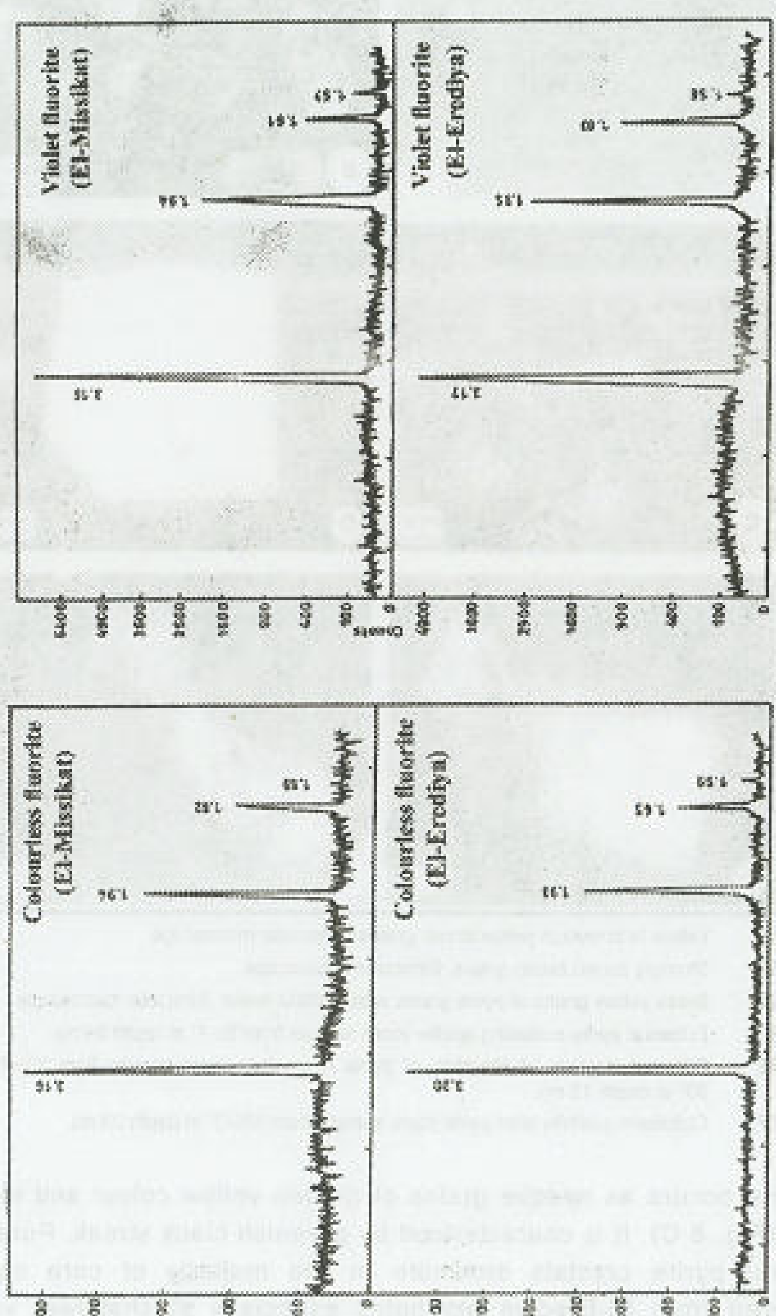

Fig.7: XRD charts for different varieties of fluorite, El-Missikat and El-Erediya plutons.

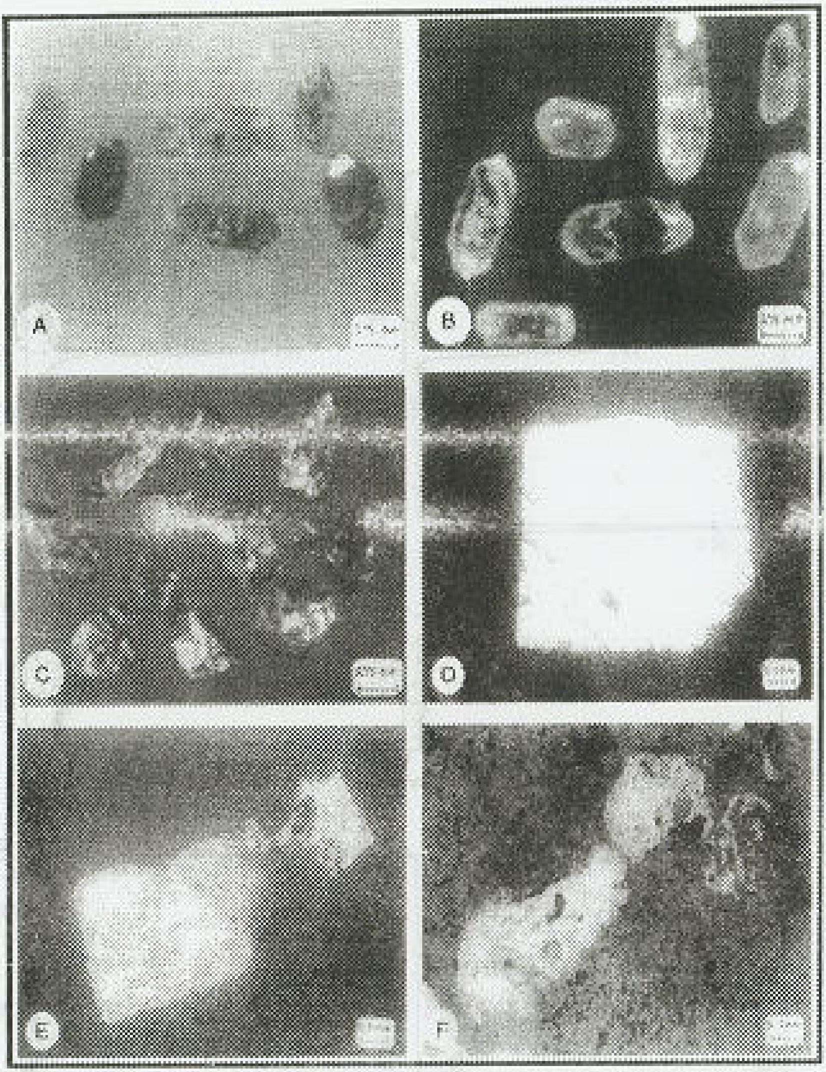

Fig. 8A: Yellow to brownish yellow zircon grains. Binocular microscope.

Fig. 8B: Strongly zoned zircon grains. Binocular microscope.

Fig. 8C: Brass yellow grains of pyrite grains with metallic luster. Binocular microscope.

Fig. 8D: Euhedral pyrite enclosing apatite (core sample from"Er-1" at depth 64 m).

Fig. 8E: Different degrees of alteration of pyrite to goethite (core sample from "Er-4M-30" at depth 12 m).

Fig. 8F: Colloform goethite after pyrite (core sample from"MS-2" at depth 23 m).

Pyrite occurs as opaque grains of golden yellow colour and metallic luster (Fig. 8 C). It is characterized by greenish black streak. Pure fresh euhedral pyrite crystals dominate in the majority of core samples recovered from El-Erediya boreholes especially at shallower vertical depths. In polished section, pyrite occurs as large euhedral to subhedral crystals. Sometimes, they are partially altered to goethite especially along fractures and grain peripheries or completely replaced by colloform goethite (Figs. 8 D, E and F).

Uranothorite occurs as deep yellowish green interstitial mineral associated with iron oxides as cracks filling in quartz or as inclusions of variable sizes and shapes within other uranium minerals. Cassiterite occurs as zoned six-sided translucent crystals associated with biotite and iron oxides.

Hematite occurs as tabular or prismatic reddish brown crystals of dull luster. They occur in compact and fibrous forms. In the mineralized granites, hematite occurs as tabular crystals in the form of aggregates of parallel orientation. Sometimes, it occurs as fine to coarse euhedral elongated crystals. The crystals are intensely fractured, curved and sheared and the twin lamellae are bent due to deformation. Hematite is usually coated or stained with a thin crust of secondary uranium minerals, especially uranophane. Sometimes, hematite is pseudomorphic after pyrite or occurs in the form of martite after magnetite or ilmenite, reflecting the hydrothermal effect.

GEOCHEMISTRY AND RADIOMETRY

El-Missikat and El-Erediya granites are nearly similar in their geochemical characteristics. Generally, they are low-Ca S-type granites slightly enriched in alkalies and depleted in Mg. They are also enriched in Rb, Y and Ba. They are considered as post orogenic granites originated from peraluminous calc-alkaline magma emplaced in a stabilizing continental crust of thickness between 20 and 30 km (Abdallah, 2004).

The altered and mineralized samples are characterized by a marked addition of SiO_2 and Fe_2O_3 which indicate the intimate relation between uranium mineralization with both silicification and hematization. The enrichment of SiO_2 and Fe_2O_3 of the altered samples is supported petrographically by the common presence of secondary quartz showing multiple phases of overgrowth and coated with iron oxides as well as the releasing of iron oxides along the cleavage planes of mica, the transformation of pyrite to goethite and the presence of metamict zircon.

Al_2O_3 and K_2O are almost subtracted indicating partial leaching during kaolinization. The depletion of K_2O indicates partial leaching of potassium during kaolinization and the partial replacement of the feldspar by the mobile K_2O during sericitization. This is supported petrographically by the common presence of cloudy and core altered feldspar. On the other hand, some trace elements such as Ga, Pb, Nb, Zr and Sr are remarkably enriched in the altered granites as compared with the fresh granites indicating the mobility of these elements.

El-Missikat and El-Erediya granites are considered as uraniferous (fertile) granites which are characterized by the following: (1) uranium contents are more than twice the Clarke value (4 ppm) whether or not they are associated with uranium mineralization, (2) eTh/eU ratios are less than 2.2, (3) SiO_2 content is more than 73 %, (4) CaO content is less than 1 %, (5) K_2O/Na_2O ratios are more than 1, (6) Zr/Sr ratios are more than 1.65, (7) Rb/Sr ratios are more than 2.5 and (8) K/Rb ratios more than 125 (Assaf *et al.*, 1997).

The distribution and variation of uranium and thorium with depth (Tables: 2 and 3) and (Fig. 9) of El-Missikat and El-Erediya boreholes reveal the following:

1- For every borehole, more than one radioactive anomaly is detected and the highest one is related to the main shear zone.

2- These radioactive anomalies are related mainly to uranium concentrations and not to thorium concentration.

3- The radioactive anomalies are not related to any of the fresh sulphide zones but mainly related to the goethite (pseudomorph after pyrite) zone.

4- The positive anomalies of uranium correspond to negative thorium anomalies.

5- There is no general trend for increasing or decreasing of either uranium or thorium with depth for any of the studied boreholes.

The above mentioned observations indicate that the magmatic differentiation plays a restricted role in uranium enrichment, meanwhile secondary processes played the principal role in the uranium enrichment of the altered granites.

Table (2): Radiometric analysis of El-Missikat and El-Erediya fresh younger granites

Pluton	Location	Sample No.	eU (ppm)	eTh (ppm)	eTh/eU
El-Missikat	Surface	1	22	64	2.91
		2	24	65	2.71
		3	18	52	2.89
		4	16	47	2.94
		5	26	31	1.19
		6	29	85	2.93
	MS-2	12	32	65	2.03
		13	25	71	2.84
		15	17	56	3.29
		17	25	72	2.88
		20	36	87	2.42
	MS-3	21	18	51	2.83
		23	26	58	2.23
		25	34	112	3.29
		28	16	66	4.13
		30	16	46	2.88
		31	22	68	3.09
Average			23.65	64.5	2.73

Pluton	Location	Sample No.	eU (ppm)	eTh (ppm)	eTh/eU
El-Erediya	Surface	32	25	79	3.16
		33	18	59	3.28
		34	15	46	3.07
		35	27	73	2.70
		36	17	55	3.24
		37	29	34	1.17
		38	21	62	2.95
	Er-1	44	30	35	1.17
		46	56	160	2.86
		48	19	43	2.26
		50	11	39	3.55
		51	18	49	2.72
		53	22	54	2.45
	Er-8M-30	54	35	116	3.31
		57	23	64	2.78
		60	11	36	3.27
	Er-7M-40	61	30	82	2.73
		64	25	72	2.88
		66	28	78	2.79
		68	23	61	2.65
		71	54	128	2.37
	Er-8M-90	72	22	51	2.32
		76	36	105	2.92
		77	53	122	2.30
Average			27	78.96	2.70

Table (3): Radiometric analysis of the percussion and altered samples of El-Missikat and El-Erediya younger granites

Location	Sample No.	eU (ppm)	eTh (ppm)	eTh/eU
Surface	7	1351	8	0.006
	8	1079	2	0.002
	9	1254	5	0.004
	10	2297	2	0.001
MS-2	11	32	37	1.16
	14	51	96	1.88
	16	849	13	0.015
	18	39	41	1.05
	19	409	8	0.02
MS-3	22	24	57	2.38
	24	24	71	2.96
	26	58	31	0.53
	27	679	4	0.006
	29	32	39	1.22
Average		584.14	34.16	0.94

Location	Sample No.	eU (ppm)	eTh (ppm)	eTh/eU
Surface	39	217	23	0.11
	40	2166	12	0.006
	41	968	9	0.009
	42	476	79	0.166
Er-1	43	1043	6	0.006
	45	34	56	1.65
	47	96	32	0.33
	49	318	17	0.05
	52	108	34	0.31
Er-8M-30	55	155	22	0.14
	56	104	16	0.15
	58	34	41	1.21
	59	56	39	0.70
Er-7M-40	62	28	61	2.18
	63	42	26	0.62
	65	157	14	0.09
	67	39	34	0.87
	69	186	21	0.11
	70	347	7	0.02
Er-8M-90	73	19	44	2.32
	74	123	15	0.12
	75	259	16	0.06
Average		316.95	28.4	0.51

Location	Sample No.	eU (ppm)	eTh (ppm)	eTh/eU
Er-8M-90 (percussion samples)	P1	22	51	2.32
	P2	36	38	1.06
	P3	19	64	3.37
	P4	28	39	1.39
	P5	13	47	3.62
	P6	21	32	1.52
	P7	41	35	0.85
	P8	32	36	1.13
	P9	35	82	2.34
	P10	19	65	3.42
	P11	31	37	1.19
	P12	17	53	3.12
	P13	23	69	3.00
	P14	24	71	2.96
	P15	14	57	1.07
	P16	39	31	0.79
	P17	26	34	1.31
	P18	45	18	0.40
	P19	16	61	3.81
	P20	28	82	2.93
	P21	33	31	0.94
	P22	18	49	2.72
	P23	18	61	3.39
	P24	38	63	1.39
	P25	31	69	2.23
	P26	23	49	2.13

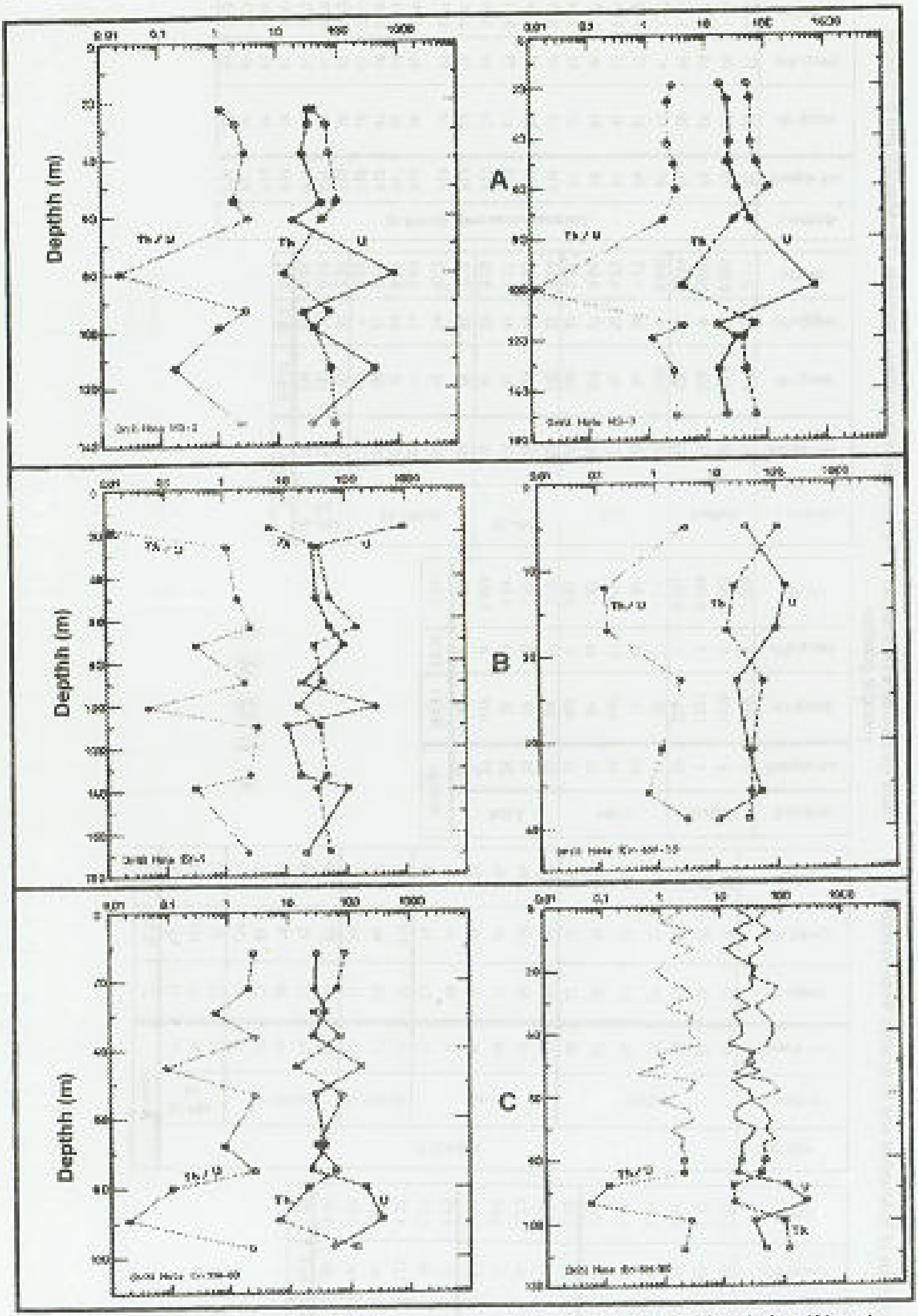

Fig.9: U and Th (ppm) and Th/U ratio versus depth (m) for El-Missikat boreholes (A) and El-Erediya boreholes (B & C)

CONCLUSIONS

According to the present study, it is concluded that there are several high subsurface radioactive anomalies in El-Missikat boreholes (MS-2 and MS-3) and El-Erediya boreholes (Er-1 and Er-7M-60). These anomalies are related to the main shear zones. Other lower radioactive anomalies are also recorded related to some fractures around the main shear zone. Although Er-4M-30 and Er-8M-90 do not intersect the main shear zone, moderate radioactive anomalies were recorded.

The radioactive anomalies are related mainly to uranium concentrations and not to thorium concentration. They are not related to any of the fresh sulphide zones but mainly related to the goethite (pseudomorph after pyrite) zone. The positive anomalies of uranium correspond to negative thorium anomalies. There is no general trend for increasing or decreasing of either uranium or thorium with depth for any of the studied boreholes. These observations reflect the secondary nature of uranium mineralizations (post magmatic ores in oxidation zones) and intimately related to shear zones as well as fracture system and accordingly to type and degree of alteration.

Uranothorite and cassiterite are only encountered in core samples at level more than 80 m depth (below the main adit level) of El-Erediya boreholes indicating a transitional area between the oxidation and reduction zones. On the other hand, they are not encountered in core samples at any depth of El-Missikat boreholes indicating oxidation zone till 150 m depth below the wadi level. It is worthy to mention that zircon ($ZrSiO_4$) and thorite ($ThSiO_4$) form a structural series with the addition of U and Th and loss in silica. The transformed zircon attains darker colour and may become opaque which is encountered as a result of invasion of hydrothermal fluids rich in U and Th. The composition of thorite is controlled by the geochemical conditions during crystallization, more than 60% of its composition is formed of ThO_2, 10% UO_2, 30% ZrO_2, Na_2O, FeO, SiO_2, Fe_2O_3, MgO, LREEs and HfO_2. The decomposition of thorite takes place in an oxidizing environment and acidic hydrothermal solutions; U replaces Th to produce uranothorite (Deer *et al.*, 1992). This concept supports the idea that the area was affected by hypogene solutions rich in U and Th.

The geochemical behavior of U and the genesis of U deposits in the studied areas could have proceeded through the following successive stages: (1) Uranium was first mainly trapped in the crystal lattice of the accessory heavy minerals of the granites, (2) The area was effected by tectonic events producing faults and shear zones which acted as good channels for the hydrothermal ascending fluids and the percolating meteoric water to mix with the trapped residual magmatic fluids rich in U and Th, and generating a low temperature hydrothermal system. This released U from the essential and accessory minerals of the hosting granites and redeposited it as uranium minerals in the shear zones.

REFERENCES

Abdallah, S. M. (1998): Subsurface geologic studies of Gabal El-Missikat uranium occurrence, Central Eastern Desert, Egypt. M.Sc. Thesis, Faculty of Science, Cairo Univ., 152 p.

Abdallah, S. M. (2004): Geological and mineralogical studies on some surface and subsurface sections from El-Missikat and El-Erediya uranium occurrences, Central Eastern Desert, Egypt. Ph.D. Thesis, Faculty of Science, Ain Shams Univ., Cairo, 219 p.

Abu Dief, A. (1985): Geology of uranium mineralization in El-Missikat area, Eastern Desert, Egypt. M.Sc. Thesis, Faculty of Science, Al-Azhar Univ., 103 p.

Assaf, H. S., Mahdy, M. A. and El Afandy, A. H. (1997): Egyptian younger granites, an approach to define parameters favouring formation of uranium deposits. 3rd Conference Geochemistry, Alexandria Univ., Egypt. pp. 409 - 420.

Bakhit, F. S. (1978): Geology and radioactive mineralization of Gabel El-Missikat area, Eastern Desert, Egypt. Ph.D. Thesis, Faculty of Science, Ain Shams Univ., Cairo, 289 p.

De la Rosa, J. D., Jenner, G. A. and Castro, A. (2002): A study of inherited zircons in granitoid rocks from the South Portuguese and Ossa-Morena Zones, Iberian Massif: support for the exotic origin of the South Portuguese Zone. Tectonophysics, vol., 352, p. 245– 256.

Deer, W.A., Howie, R.A. and Zussmann, J. (1992): An introduction to the rock forming minerals. Longmans, London. 696 p.

El-Kassas, I. A. (1974): Radioactivity and geology of Wadi Atalla area, Eastern Desert of Egypt. Ph.D. Thesis, Faculty of Science, Ain Shams University, Cairo, 502 p.

El-Mansi, M. M. (1993): Petrology, radioactivity and mineralizations of Abu Gerida El-Erediya area, Eastern Desert, Egypt. M. Sc. thesis, Faculty of Science, Cairo University, Cairo, Egypt, 223 p.

El-Mansi, M. M. (2000): Colouration of fluorite and its relation to radioactivity. Jour. Min. Soc. Egypt. Vol. 12, 12 p.

Holten, T., Jamtveit, B. and Meakin, P. (2000): Noise and oscillatory zoning of minerals. Geochim. Cosmochim. Acta, vol. 64 (11) p. 1893-1904.

Moharem, A. F. (2000): Geology, geochemistry and radioactivity of some granitic masses in the area of Gabal El-Maghrabiya, Central Eastern Desert, Egypt. Ph.D. Thesis, Faculty of Science, Ain Shams Univ., 190 p.

Nagi, R. M. (1977): Geochemistry of the Rie El-Garra pluton, Egypt. Ph.D. Thesis, Rice Univ., U.S.A., 73 p.

Omran, A. A. (1999): Subsurface geologic studies of Gabal El-Eredyia uranium occurrence, Central Eastern Desert, Egypt. M.Sc. Thesis. Faculty of Science, South Valley Univ., Qena, 136 p.

Rabie, S. I. and Ammar, A. A. (1992): Schematic relief of the near-surface and deep-seated magnetic basement, using local power spectra Gabal El-Erediya area, Eastern Desert, Egypt. J. Afr. Vol. 14, No.1, pp. 147 - 152.

Raslan, M. F. (2001): Mineralogical and physical separation studies on some radioactive granites from the Eastern Desert, Egypt. Ph. D. Thesis Faculty of Science, Cairo University, 204 p.

Salman, A. B. (1995): Proposed exploratory diamond drilling programme for El-Missikat uranium occurrence. Internal report, Production Sector, N.M.A., 3 p.

دراسات معدنية وتوزيع اليورانيوم فى بعض القطاعات التحت سطحية لتواجدات اليورانيوم من منطقتى المسيكات والعرضية، الصحراء الشرقية، مصر

عبد المنعم محمد عثمان*- عبد العاطى بدر سالمان**- مدحت محمود المنسى**- إسماعيل محمد عبد الغنى**- سمير محمد عبد الله**

* كلية العلوم - جامعة عين شمس – القاهرة – مصر .

** هيئة المواد النووية – القاهرة – مصر .

قامت هيئة المواد النووية بتنفيذ برنامج للحفر اللبى والقناتى والذى تم من خلاله حفر مجموعة من الآبار الإستكشافية ذات أعماق وميول مختلفة اثنان منها بمنطقة المسيكات وعشرة بمنطقة العرضية. وبدراسة البئرين (MS-2 ، MS-3) من منطقة المسيكات وكذلك أربعة آبار من منطقة العرضية (Er-1 ، Er-4M-30 ، Er-7M-60 ، Er-8M-90) اتضح تواجد بعض الشاذات الإشعاعية العالية والتى تنتمى إلى نطاق التكسر والتهشم الرئيسى علاوة على بعض الشاذات الإشعاعية القليلة نسبياً والتى ترتبط ببعض الشقوق حول نطاق التكسر الرئيسى.

وقد تبين أن هذه الشاذات الإشعاعية مرتبطة أساساً بتمعدنات اليورانيوم وليست الثوريوم كما أنه لا علاقة لها بنطاقات معادن الكبريتيدات الطازجة بل بنطاقات معدن الجوثيت الناتج عن أكسدة البيريت. وأنه لايوجد اتجاه محدد للزيادة أو النقصان سواء لليورانيوم أو الثوريوم مع العمق فى أى من الآبار التى تم دراستها علاوة على أن تمعدنات اليورانيوم ذات طبيعة ثانوية ولها علاقة وطيدة بنطاقات التكسر ونظم التشقق وكذلك على نوع ودرجة التحلل.

وقد وجد أن معدنى اليورانوثوريت والكاسيتيريت موجودة فى بعض العينات اللبية على أعماق أكبر من ٨٠ متر أسفل مستوى الممر الرئيسى للمنجم الإستكشافى فى جبل العرضية دلالة على أن هذا النطاق فاصل بين نطاقى التأكسد والإختزال على عكس جبل المسيكات لم يتم العثور على أى من هذين المعدنين مما يؤكد استمرار نطاق التأكسد حتى عمق ١٥٠ متر أسفل مستوى الوادى.